

Types, Petrophysical Properties and Pore Evolution of Late Ediacaran Microbial Carbonates, Tarim Basin, NW China



1922—2022

TANG Pan^{1,2,3}, CHEN Daizhao^{1,2,3,*}, QIAN Yixiong⁴, WANG Yuanzheng^{1,2,3} and YANG Bo^{1,2,3}

¹ Key Laboratory of Cenozoic Geology and Environment, Institute of Geology and Geophysics, Chinese Academy of Sciences, Beijing 100029, China

² Innovation Academy for Earth Science, Chinese Academy of Sciences, Beijing 100029, China

³ University of Chinese Academy of Sciences, Beijing 100049, China

⁴ Wuxi Research Institute of Petroleum Geology, SINOPEC, Wuxi, Jiangsu 214151, China

Abstract: The Upper Ediacaran microbial carbonates of the Tarim Basin are potential reservoir geobodies for future hydrocarbon exploration with rising interest in exploration for deeply-buried reserves. However, little knowledge has been acquired on the types of microbial carbonates that are present, the properties of the reservoir and the pore evolution, hampering predictions of high-quality reservoirs in these carbonates. Integrated with petrography and in-situ U-Pb dating geochronology analyses, this study aims to clarify the types of microbial carbonates present and to reconstruct the pore evolution processes of the potential reservoir rocks. The Upper Ediacaran microbial carbonates of the Tarim Basin can be divided into four types, based on their features in terms of different scales (macro- to micro-): microbial laminites, stromatolites, spongiomicrobialites and microbial-peloidal wackestone/mudstone. Petrophysical properties show that all these microbial carbonates have low porosity and very low permeability with poor connectivity. These carbonates were subject to long-term and complex diagenetic processes, mainly consisting of dissolution, compaction, pervasive dolomitization, cementation and fracturing. The most important reservoir spaces are contributed by vugs and dissolution-enlarged pores, which are likely to have been associated with the widespread uplift of the Aksu area in the terminal Ediacaran. In contrast, the cementation of the fine-to-medium crystalline dolomite greatly reduced the pre-existing pores. Pore types are closely related to different microbial fabrics, which played an important role in the pore evolution of the microbial carbonates.

Key words: microbial carbonate, Late Ediacaran, reservoir property, pore evolution, Tarim Basin

Citation: Tang et al., 2022. Types, Petrophysical Properties and Pore Evolution of Late Ediacaran Microbial Carbonates, Tarim Basin, NW China. *Acta Geologica Sinica (English Edition)*, 96(4): 1362–1375. DOI: 10.1111/1755-6724.14974

1 Introduction

Microorganisms (e.g., cyanobacteria, algae and fungi) are widely distributed on Earth's surface throughout both geological history and the present (Hofmann, 1973; Riding, 2011; Couradeau et al., 2012). They have played important roles in the precipitation of carbonate sediments (Seckbach and Oren, 2010; Chen and Lee, 2014). As in situ precipitates produced by the physiological activity of benthic microorganisms, microbial carbonates (also called microbialites) are defined as organosedimentary deposits formed by the interactions between microbial communities and environments (Burne and Moore, 1987; Kenter et al., 2005). In the petroleum industry, it has been demonstrated that microbial carbonates have the potential capacity to host large volumes of oil and gas. With recent discoveries of hydrocarbons in microbial carbonates, as those reported in the Siberian Platform of Russia, the Precaspian Basin of Kazakhstan and the Santos Basin of Brazil (Tull, 1997; Collins et al., 2006; Muniz and Bosence, 2012), interests in these microbial reservoirs are increasing. In China, high-

quality microbial carbonate reservoirs have been discovered in the Tarim Basin, the Sichuan Basin and the North China Platform, which could also serve as promising geobodies to be targeted for exploration (Zhang et al., 2017; Jiang et al., 2018; Zhu et al., 2020, 2021; Li Y et al., 2021).

With drilling penetrating to a greater depth than before in the Tarim Basin, 2020 saw exploration well LT-1 acquire natural gas at a depth from 8737 m to 8750 m in the Upper Ediacaran Qigebrak Formation, dominated by microbial carbonates, indicating exploration potential in Precambrian microbialites (Yang H J et al., 2020). Although, previous studies on the Qigebrak Formation have dealt with the classification of these microbial carbonates (Li et al., 2015; Yang et al., 2017; Li F et al., 2021), there remains considerable debate concerning the types of Late Ediacaran microbial carbonates present in the Tarim Basin. In addition, porosity formation and preservation, as well as the petrophysical properties of the different microbial carbonates, are still unclear, hindering understanding of the formation mechanism and undermining predictions of related high-quality reservoirs.

In this study, based on a comprehensive analysis of outcrop and drilling samples, it is intended to clarify the

* Corresponding author. E-mail: dzh-chen@mail.iggcas.ac.cn

types of microbial carbonates present, with respect to their depositional environments, then link the petrophysical properties to diagenetic events and pore evolution processes, ascertaining the key factors controlling pore creation or destruction during diagenesis. Specifically, the following questions will be addressed:

(1) How many types of microbial carbonates are present in the Late Ediacaran of the Tarim Basin and what are their petrological characteristics?

(2) Which type of microbial carbonates have the best reservoir potential?

(3) What is the relationship between microbial fabrics and pore evolution?

2 Geological Setting

The Tarim Basin is regarded as an intracratonic basin,

bordered by the Tianshan Mountains on the northern side, the Kunlun Mountains on the southwestern side and the Algn Mountains on the southeastern side (Jia, 1999; Fig. 1a). The tectonic evolution of the Tarim Basin in the Precambrian was closely related to the assembling-disassembling cycle of the Columbia and Rodinia supercontinents (He et al., 2005; Zhai, 2013). The Tarim Block was detached from NW Australia during a pervasive rifting event that occurred during the late Neoproterozoic (Li and Powell, 2001). Continental rift basins were developed in the margin and interior of the Tarim block (Basin), due to extensional processes spanning from the Cryogenian to the Early Ediacaran, which resulted in over 1000 m thick clastic deposits interbedded with volcanic rocks (Turner, 2010). In the Late Ediacaran, the continuous expansion of the rift evolved to flexural subsidence in the ocean basin, forming

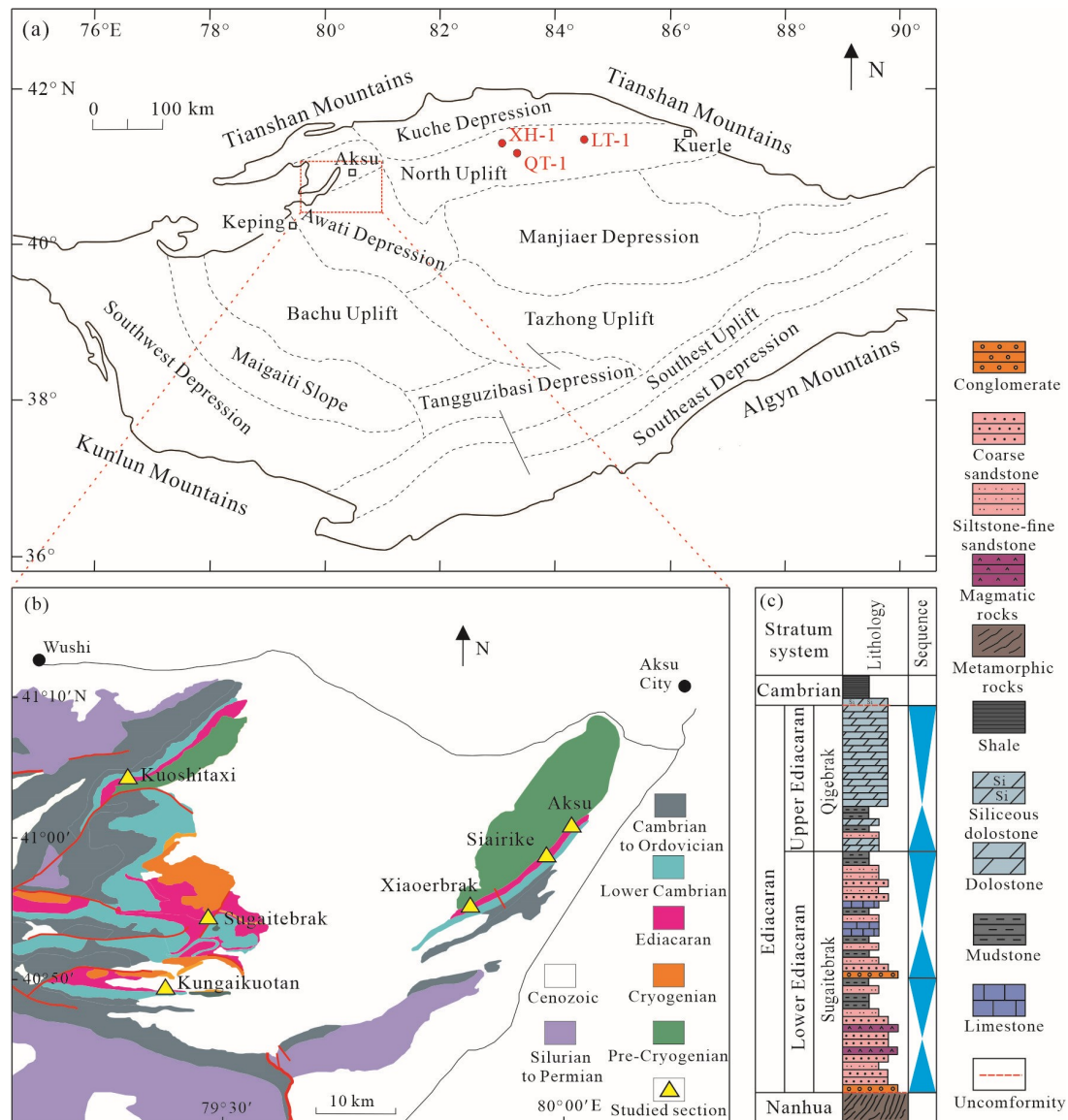


Fig. 1. (a) General structural units and location of the Tarim Basin. Rectangle outlined in red shows the Aksu area, modified from Zhu et al. (2015); (b) geological map of the Aksu area, yellow triangles show locations of studied sections, modified from Zhou et al. (2014); (c) simplified stratigraphic column from the Ediacaran to Lower Cambrian in the NW Tarim Basin, modified from Shi et al. (2016).

a flexural basin characterized by the occurrence of shallow epicontinental marine carbonates (Turner, 2010; Wu et al., 2017). During the Phanerozoic, however, the Tarim Basin was subject to multiphase tectonic events and deformational orogenies (Caledonian, Hercynian, Indosinian and Himalayan), forming various tectonogeomorphological units within the subsurface (Jia, 1999; Fig. 1a).

The six studied outcrop sections are located near the city of Aksu (Fig. 1b). The Ediacaran strata in the NW Tarim Basin comprises the Sugaitebrak and Qigebrak formations, in ascending order (Fig. 1c). The Qigebrak Formation conformably overlies the Lower Ediacaran Sugaitebrak Formation clastic rocks, in its turn unconformably overlain by the bedded cherts and black shales of the Cambrian Yuertusi Formation (Fig. 1c), with a total thickness of less than 200 m (Fig. 2). During the deposition of the Qigebrak Formation (Late Ediacaran), the study area was mostly occupied by the tidal flat of a restricted carbonate platform (Wu et al., 2017), although rimmed with microbial (i.e., columnar stromatolite) reefs

in the later part of the interval. The main lithofacies in the Qigebrak Formation, in order of decreasing volume percentage, include dolomitized microbial carbonates, dolowackestone/dolomudstone, dolograinstone and minor sandstone, of which microbial carbonates account for over 75% by volume (Fig. 2). By the end of the Ediacaran period and owing to either regional tectonic movement or a large-scale sea level fall (Lin et al., 2012; He et al., 2018), the uppermost Qigebrak Formation was subject to extensive subaerial exposure and karstification, forming an extensive unconformity surface (Fig. 2), under which karstic brecciation/collapse, dissolution pipes/cavities or vugs are common, although also experiencing intense subsequent hydrothermal silicification (Zhou et al., 2014).

3 Materials and Methods

This study is based on observation of field outcrops and the analysis of 345 samples collected from the six sections (Kuoshitaxi, Sugaitebrak, Kungaiquotan, Xiaoerbrak, Aksu and Siairike) in the Aksu area as well as two drilling

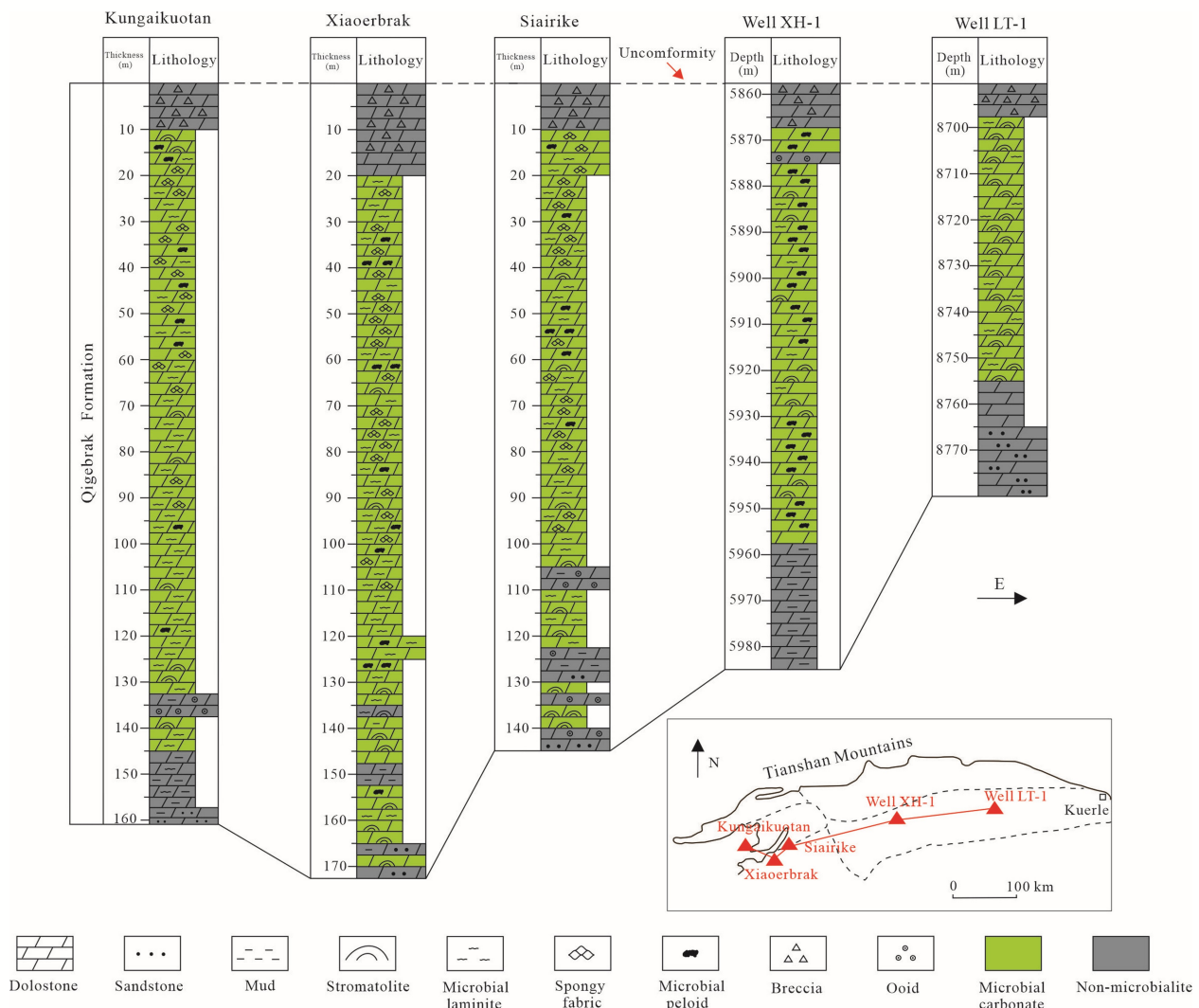


Fig. 2. Stratigraphic column of the Qigebrak Formation in the northern Tarim Basin.

wells (LT-1 and XH-1). Petrographic observation was carried out to identify the types of microbial carbonates, through specifying the nature and presence of microbial fabrics such as laminae and spongy textures. The classification of microbial carbonates follows the nomenclature of Dunham (1962) and Embry and Klovan (1971), combined with the description scales of microbial structures (mega-, macro-, meso- and micro-) proposed by Shapiro (2000).

Representative samples were selected for microscopic petrographical observation, including optical transmitted light and scanning electron microscopy (SEM), which were conducted at the Institute of Geology and Geophysics, Chinese Academy of Sciences (IGGCAS). 95 polished thin sections were impregnated with blue resin in order to better observe the pores. 10 samples were chosen for examination of mineral morphological characteristics and spacing, using a Nova NanoSEM 450. The operating conditions included an accelerating voltage of 15 kV, a working distance of 6–6.5 mm and a tilt angle of 0°.

In order to investigate petrophysical properties of different microbial carbonates, a helium test was performed to characterize the porosity and permeability of the 116 obtained plug samples. In addition, following the criteria and steps proposed by Zhang et al. (2014), point counting was conducted to determine the visual porosity of the thin sections.

4 Results

4.1 Types of microbial carbonates

Riding (2000) proposed that microbial carbonates can be divided into four distinct types: stromatolite, thrombolite, dendrolite and leiolite. In the microbialite-bearing successions of the Tarim Basin, Sichuan Basin and North China platform, stromatolites (laminated structure) and thrombolites (clotted structure) are generally more widely recognized than other types (Chen et al., 2019; Li F et al., 2021). In the studied area, linking the microbial fabrics and components with their associated

depositional environments, four types of microbial carbonates are distinguished from the Qigebrak Formation. Figure 3 summarizes the features (sedimentary features, main components, morphology, water energy and depositional environment) of each type.

4.1.1 Microbial laminite

This type is widely distributed in all the studied outcrop sections, especially in the lower and middle parts of the Qigebrak Formation (Fig. 2). Volumetrically, it accounts for roughly 30% of the microbial carbonate rocks. Microbial laminite is generally dark gray in color and thin-to-medium bedded (Fig. 4a). Planar laminae dominate, represented by mm to cm scale lamination, illustrated by the alternation of filamentous and micro-peloidal laminae (Fig. 4a). These laminae are generally considered to be the result of microbial metabolism related to mineral precipitation, involving the trapping and binding of sediment particles (Riding, 2000; Bahniuk et al., 2015). Fenestral fabrics (Fig. 4b) and internal sediments are developed between laminae. Fibrous dolomite cements (Fig. 4b) locally occur in some fenestral pores. This type of microbial carbonate represents deposits of flat-lying microbial mats, mainly deposited in intertidal to supratidal flats with low water energy (Fig. 3).

4.1.2 Stromatolite

This type accounts for approximately 16.5% of the microbial carbonates in total. Stromatolite is gray to dark gray and medium-thick bedded commonly, with three types of stromatolites being identifiable in macro- to meso- scale: wavy, domal and columnar (Figs. 3, 4c–f). Domal stromatolites usually occur in association with wavy stromatolites vertically (Fig. 4d), the thickness of laminae ranging from submillimeter to 1.5 millimeters in scale (Fig. 4e). The alternation of dark and light dolomite intervals most likely reflects changes of organic content. For columnar stromatolites, individual columns are typically 5–25 cm in diameter and 30–200 cm in height (Fig. 4f), which locally occur in the upper Qigebrak

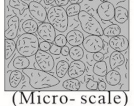
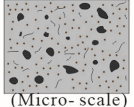
Microbial carbonate types	Sedimentary features	Main components	Morphology	Water energy		Supratidal	
				Low	High	Intertidal	Subtidal
Microbial laminite	Planar laminae dominant, fenestral fabrics locally occur	Dolomicrite, peloids and dolosparite	 (Macro- to Meso- scale)	-----	-----	-----	-----
Stromatolite	Columnar, domal to wavy structures	Dolomicrite, peloids and dolosparite	Wavy  Domal  Columnar  (Macro- to Meso- scale)	... ---	... ---	... ---	... ---
Spongiomicrobialite	Fenestral fabrics locally occur	Dolomicrite and dolosparite	 (Micro- scale)	-----	-----	-----	-----
Microbial-peloidal wackestone/mudstone	Leiolite-like structure in macro- scale	Microbial peloids and muddy dolomicrite matrix	 (Micro- scale)	-----	-----	-----	-----

Fig. 3. The main features of different microbial carbonates in the Qigebrak Formation.

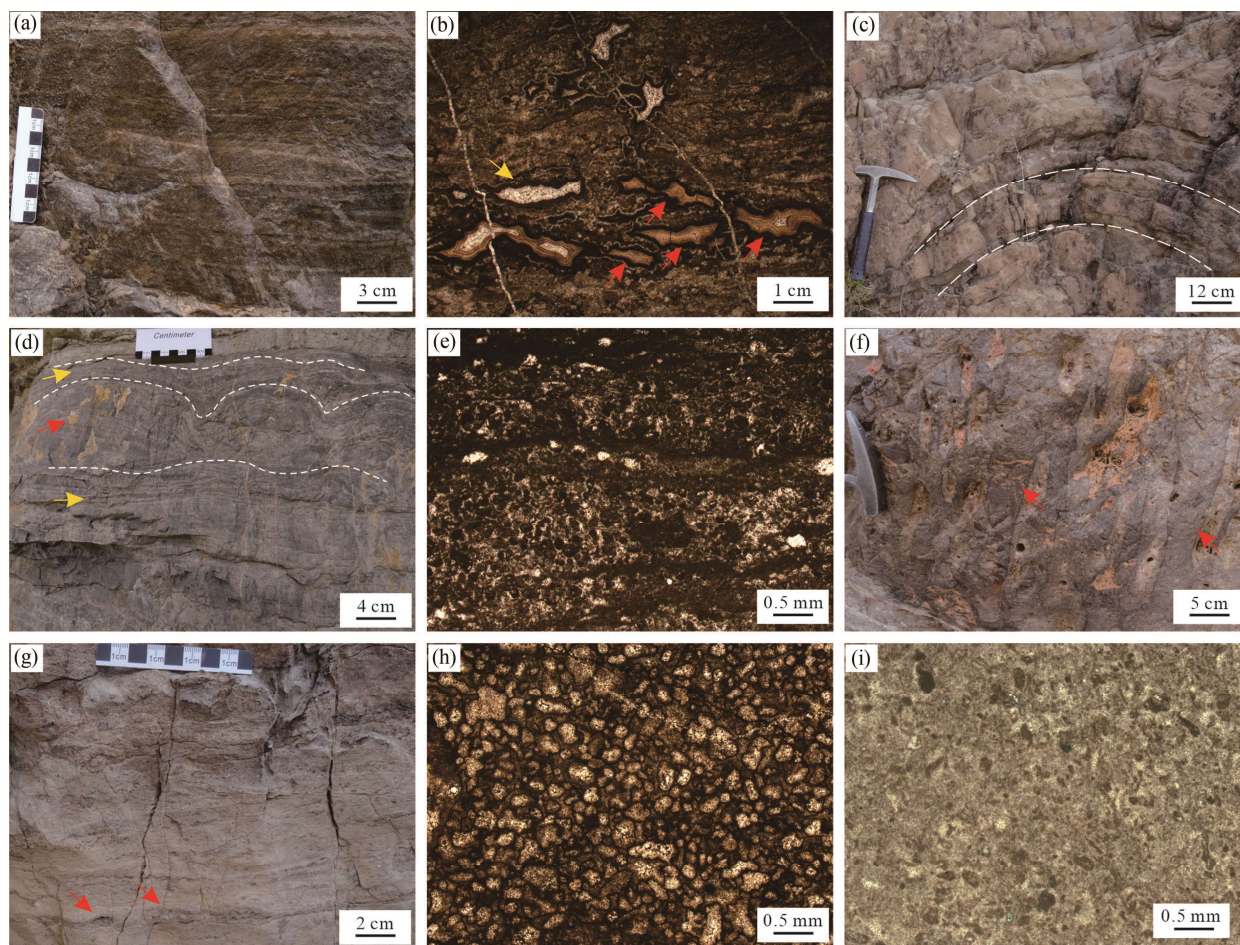


Fig. 4. Various types of microbial carbonates in the Qigebrak Formation. All photomicrographs were taken under plane-polarized light. (a) Microbial laminite with planar laminae, outcrop, Siairike section; (b) fenestral fabrics (yellow arrow) and fibrous cements (red arrow) are developed between the laminae of microbial laminite, thin-section, Xiaerbrak section; (c) domal stromatolites, height about 20 cm, outcrop, Kungaiquotan section; (d) domal stromatolites (red arrow) occur associated with wavy stromatolites (yellow arrow) vertically, outcrop, Xiaerbrak section; (e) stromatolite with coarse laminae and peloids, thin section, Siairike section; (f) columnar stromatolite (red arrow) with a lot of unfilled vugs, height about 50 cm, outcrop, Kuoshitaxi section; (g) spongiomicrobialite with fenestral fabrics filled by fibrous cements (red arrow), outcrop, Kungaiquotan section; (h) spongiomicrobialite, the rims of the spongy fabrics were micritized, thin section, Siairike section; (i) microbial-peloidal wackestone, thin section, Aksu section.

Formation. They have mm-scale domal to wrinkly laminae, similar to that of wavy/domal stromatolites.

Columnar, domal and wavy structures in stromatolites are considered to be a reflection of water energy conditions from high to low, respectively (Flügel, 2010; Fig. 3). Columnar stromatolites are commonly constructed upwards and bound laterally as the reef (build ups) rimming the platform margin, so that they possess the solid framework necessary to resist high energy current washing/agitation. The domal to wavy stromatolite morphologies are supposed to have been formed in the shallow subtidal-to-intertidal zone (Ding et al., 2019a; Fig. 3), where the water energy was higher than the shallower intertidal flat, colonized by microbial mats (Kah et al., 2006; Harwood and Sumner, 2011).

4.1.3 Spongiomicrobialite

Volumetrically, this type of microbial carbonate constitutes nearly 38.3%, mainly developed in the middle and upper part of the Qigebrak Formation (Fig. 2). Spongiomicrobialite, light gray in color and medium-to-

thick bedded, is characterized by weak, sparsely discontinuous or even absent laminae and clots in the macro or meso scale, similar to the leiolite-like structure in some cases (Braga et al., 1995; Fig. 4g). In thin sections, a single spongy fabric is characterized by an oval or subrounded chamber/coelome with a size between 0.1 mm and 0.6 mm, lined by dolomicrite to fine crystalline dolosparite from margin to coelome (Fig. 4h). The formation of a spongy fabric framework was possibly related to the mineralization of cyanobacteria (Li et al., 2015). Fenestral fabrics occur locally (Fig. 4g). This type was likely deposited from intertidal to shallow subtidal flat settings, with low-moderate water energy (Fig. 3).

4.1.4 Microbial-peloidal wackestone/mudstone

This type constitutes 15.2% of all the microbial carbonates by volume, developed locally in the Qigebrak Formation. It is commonly gray to dark gray, thin-to-medium bedded. They generally display leiolite-like structures with an absence of distinct laminae in the outcrop, similar to an extent to that of

spongiomicrobialite. Major components include microbial peloids and muddy dolomicrites (Figs. 3, 4i). The microbial peloids vary from 0.05–0.2 mm in size (Fig. 4i). The clotted fabric of the micropeloids and the occurrence as constituents of bindstones point to a microbially-induced origin of these grains, formed in situ within mats, which were biochemically precipitated, triggered by microbes and organic substances (Flügel, 2010). The large number of dolomicrites and the absence of exposure sedimentary fabrics suggest that this type was deposited in a relatively low-energy environment, from subtidal to intertidal flat (Tucker and Wright, 1990; Fig. 3).

4.2 Petrophysical properties

Helium test data of the 116 samples from the studied sections show that the microbial carbonates in the Qigebrak Formation generally have low porosity and very low permeability (Fig. 5). Among these types, stromatolite and spongiomicrobialite have a relatively high average porosity (4.82% and 6.15%, respectively; Fig. 5). The average porosity of microbial laminite and microbial-peloidal wackestone/mudstone are quite close (4.09% and 3.96%, respectively) and lower than those of stromatolite and spongiomicrobialite. Relative to average permeability, all four types have a narrow range, varying from 0.102 mD to 0.201 mD (Fig. 5).

More specifically, the predominant range of porosity in each type varies a lot (Fig. 6a, c, e, g). For microbial laminite, nearly 70% of the samples have porosity ranging from 2% to 6%. For stromatolite, nearly 50% of the samples have porosity 0–2% and 4%–6%. The porosity of spongiomicrobialite is relatively high, over 50% of the samples have porosity between 6% and 10%, some having porosity up to 10%–12%. In contrast, the microbial-peloidal wackestone/mudstone has poor reservoir potential, over 40% of the samples having a porosity less than 2%. The range of permeability of these microbial carbonates does not show a big difference (Fig. 6b, d, f, h), most samples yielding permeability between 0.001mD and 1 mD, only a few samples (less than 10%) having relatively high permeability (1mD to 10 mD).

In summary, stromatolite and spongiomicrobialite

possibly have better reservoir properties than the other two types, of which the spongiomicrobialite has the best reservoir potential. Well-logging interpretation from well LT-1 reveals that the thickness of class I reservoirs (porosity higher than 4.5%) and class II reservoirs (porosity between 2.5% and 4.5%) are 28.5 m and 9 m, respectively, for which the average porosity is 4.0% (Yang H J et al., 2020). Additionally, high-quality reservoirs are mainly distributed in the upper part of the Qigebrak Formation, the thickness for natural gas production being about 13 m, the reservoir rocks being dominated by stromatolites and spongiomicrobialites (Yang H J et al., 2020). Reservoir properties from well LT-1 are consistent with those of the studied sections, showing the microbial carbonates of the Qigebrak Formation have the potential to be high-quality reservoirs.

4.3 Diagenetic features

4.3.1 Dissolution

Various types of pores are products of multistage dissolution. Reservoir spaces of microbial carbonates are dominated by secondary pores, including vugs and dissolution-enhanced pores (Figs. 4f, 7a). They are non-fabric selective with irregular to rounded shapes, characterized by the harbor-like embayments at the edge (Fig. 7a). Primary pores were locally developed and contributed less to total porosity, including fenestral pores (Fig. 7b), part of the spongy fabric related pores (Fig. 7c) and lacy framework pores (Fig. 7d–e). Other pore types such as intercrystalline pores (Fig. 7b) and micropores (Fig. 7f) are commonly observed, even though they only make a limited contribution to reservoir spaces. Refer to Table 1 for an overview (size, occurrence and point-counting porosity) of different pore types.

4.3.2 Compaction

Mechanical compaction and pressure dissolution (i.e., chemical compaction) are developed in the Qigebrak Formation. In ooidal grainstone intervals, many ooids have a ductile elliptical shape and sometimes grain-to-grain compaction (Fig. 8a), indicating that the Qigebrak Formation has experienced intense physical compaction during the burial phase, which has resulted in substantial

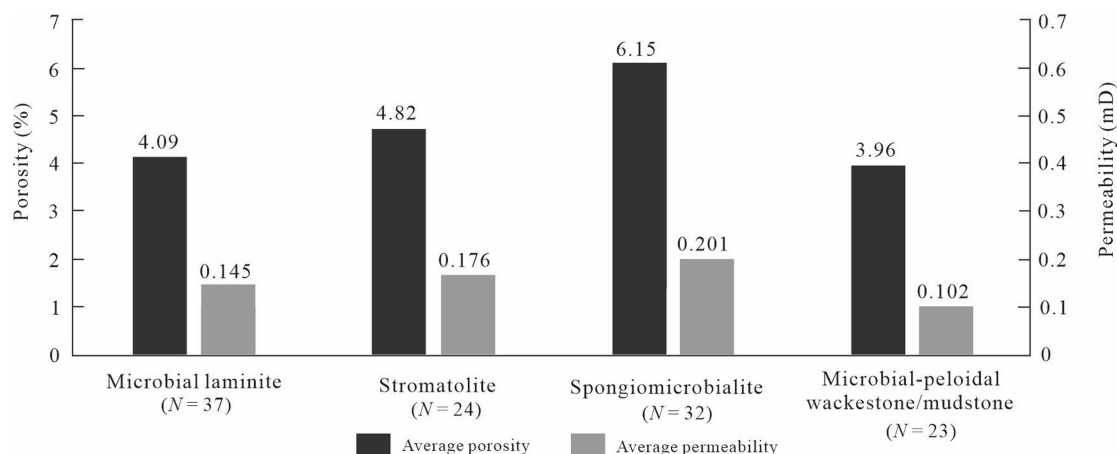


Fig. 5. Histogram of average porosity and average permeability of various microbial carbonates in the Qigebrak Formation.

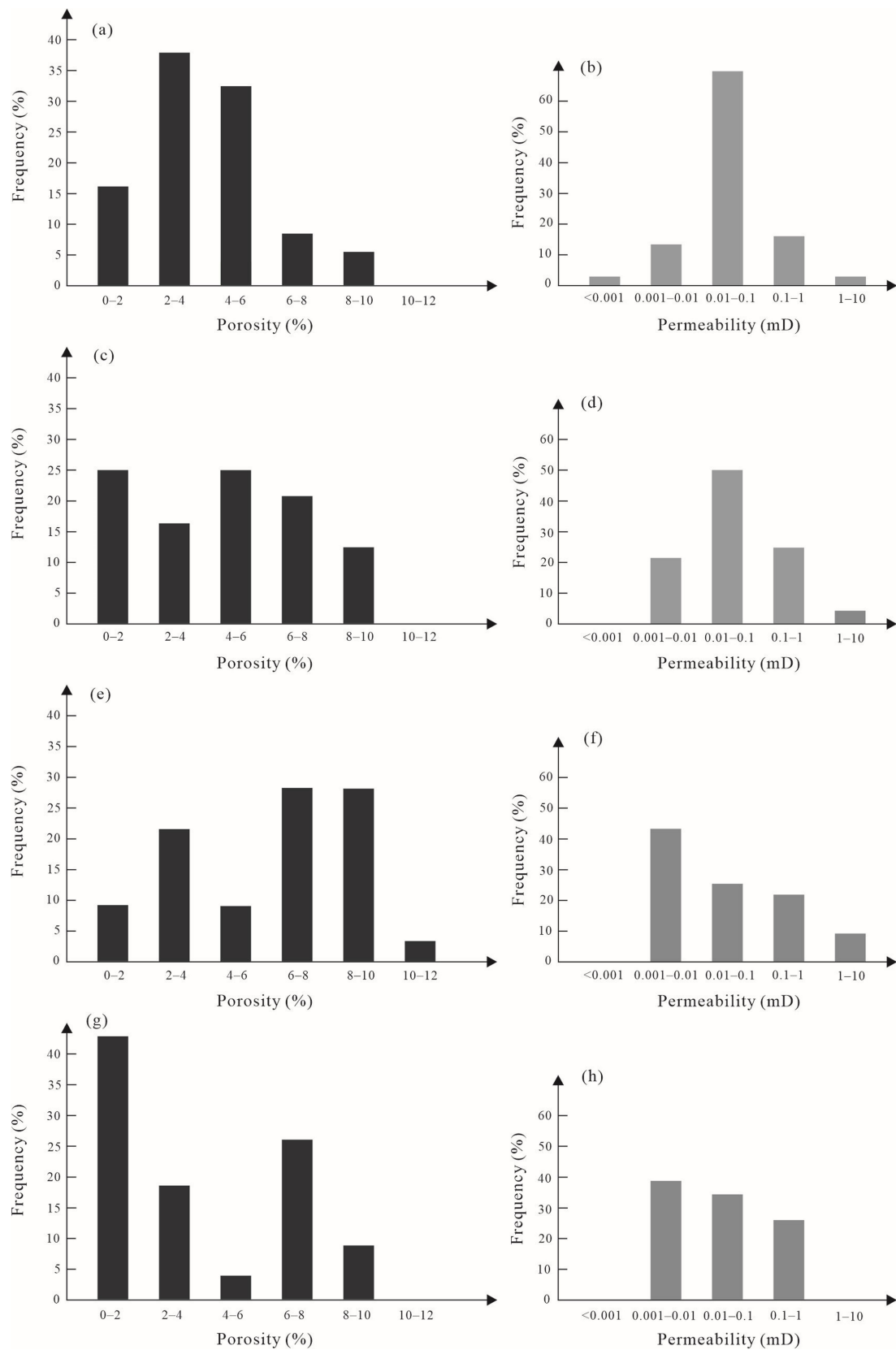


Fig. 6. Histograms showing the range of porosity and permeability of different microbial carbonates in the Qigebrak Formation. (a) and (b) for microbial laminites; (c) and (d) for stromatolite; (e) and (f) for spongiomicrobialite; (g) and (h) for microbial-peloidal wackestone/mudstone.

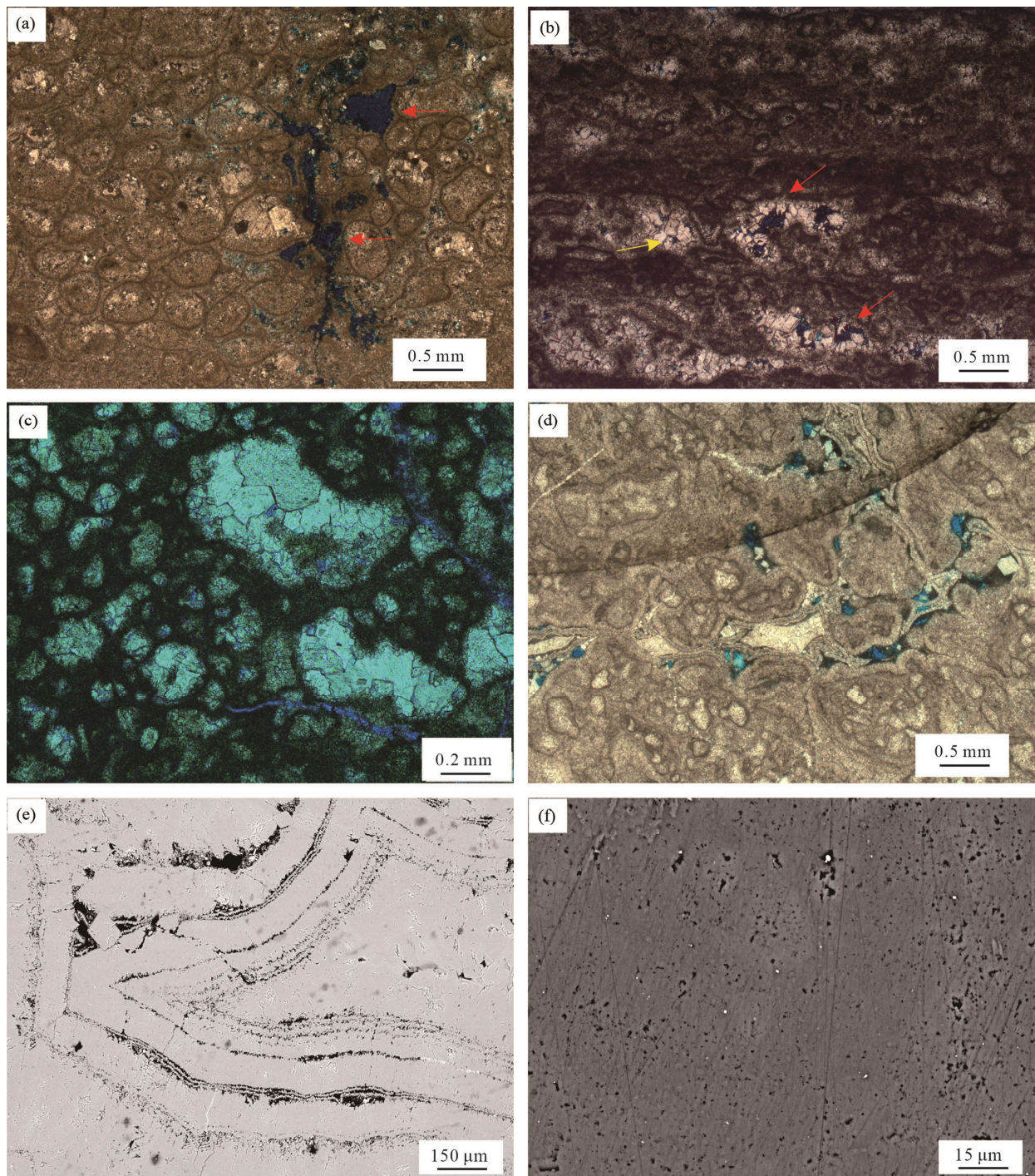


Fig. 7. Various pore types of microbial carbonates in the Qigebrak Formation.

(a) Vugs and dissolution-enhanced pores (red arrow) have harbor-like shapes, dissolution was non-fabric selective, Aksu section; (b) fenestral pores (red arrow) are partially filled by dolomite cements, intercrystalline pores (yellow arrow) occur between dolomite crystals, Siairike section; (c) spongy fabric-related pores are well-developed in the spongiomicrobialite, well QT-1, depth 6004 m; (d) lacy framework pores developed and partially filled by fibrous dolomite cements, Kungaiquotan section; (e) BSEM image showing lacy framework pores, Xiaocerbrak section; (f) BSEM image showing abundance of micropores, Sugaitebrak section.

porosity loss. Stylolites are less common and usually have low amplitudes, commonly being filled with bitumen and/or clay minerals (Fig. 8b).

4.3.3 Pervasive dolomitization

The studied microbial carbonates have been completely

dolomitized after deposition of microbial mats. In the matrix, microbial dolomicrites are predominant diagenetic minerals, with aphanocrystalline to very finely crystalline (Fig. 8b–c). Previous study has shown that $\delta^{13}\text{C}$ and $^{87}\text{Sr}/^{86}\text{Sr}$ values of these matrix dolomites lie in the range of estimated Late Ediacaran coeval seawater and indicates

Table 1 Summary of pore types in the microbial carbonates from the Qigebrak Formation

Pore type	Pore size	Pore occurrence	Point-counting porosity
Vugs and dissolution-enhanced pore	Mostly 100 to 500 μm , up to several millimeters	Spongiomicrobialite, Stromatolite and microbial-peloidal wackestone/mudstone	5–10%
Fenestral pore	10 to 200 μm	Microbial laminite and stromatolite	2–6%
Spongy fabric-related pore	10 to 500 μm	Spongiomicrobialite	5–10%
Lacy framework pore	5 to 250 μm	Spongiomicrobialite and stromatolite	2–8%
Intercrystalline pore	5 to 50 μm	Microbial laminite, stromatolite, Spongiomicrobialite and microbial-peloidal wackestone/mudstone	2–5%
Micropore	Less than 5 μm	Microbial laminite, stromatolite and spongiomicrobialite	Minor, less than 2%

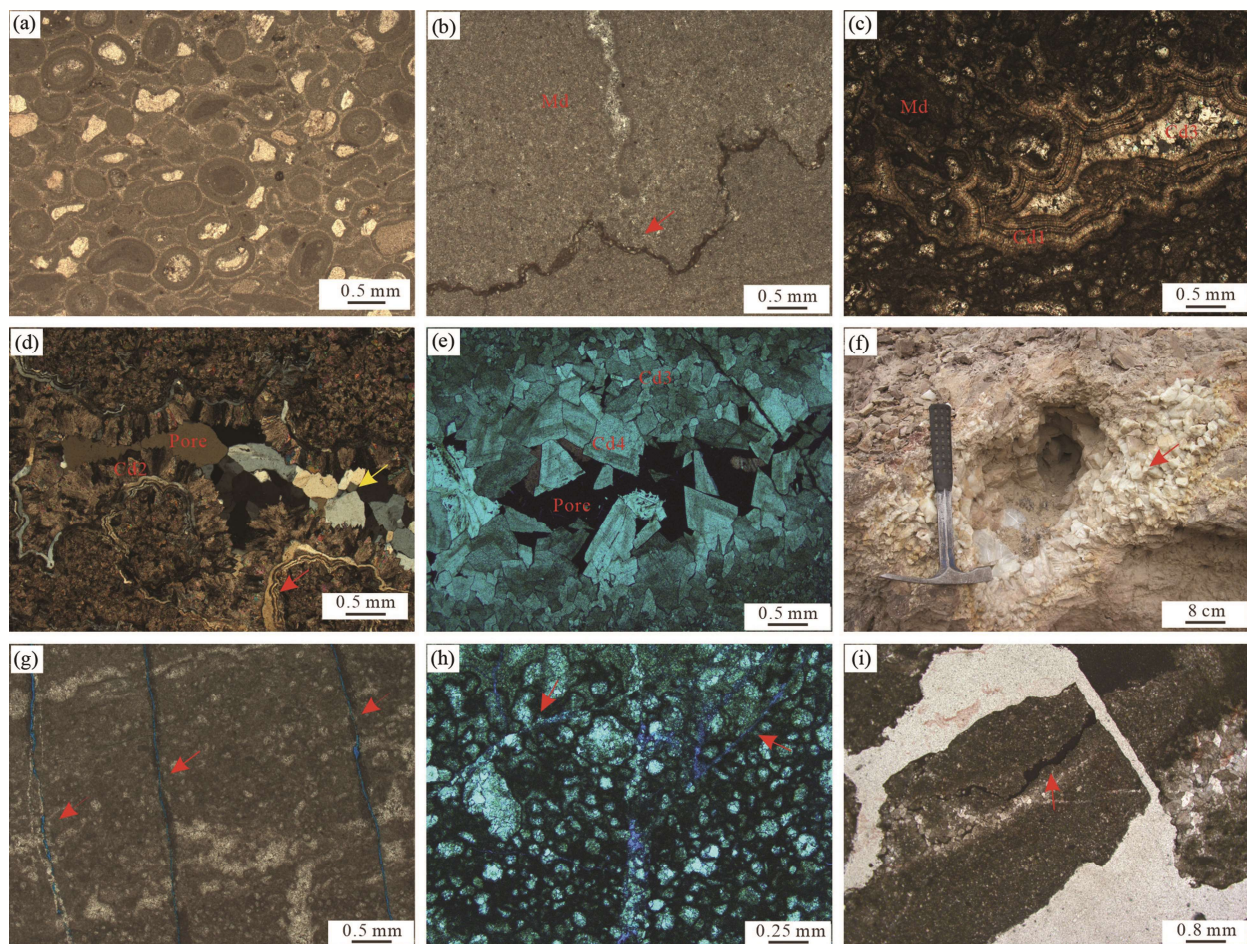


Fig. 8. Main diagenetic features in the Qigebrak Formation.

(a) Ooids and peloids are tightly packed and have elliptical shape, Kuoshitaxi section; (b) low-amplitude stylolite (red arrow) filled with clay minerals and bitumen, Kuoshitaxi section; (c) spongy fabric with pores filled with Cd1 and Cd3, Xiaerbrak section; (d) pores filled with Cd2, early-stage chalcedony (red arrow) and late-stage quartz (yellow arrow), Siairike section; (e) pores filled with Cd3 and Cd4, well QT-1, depth 6000 m; (f) karst cave with megacrystalline calcite infill, Aksu section; (g) grouped unfilled tectonic fractures (red arrow) in stromatolite, Kungaikuotan section; (h) multiphase unfilled microfractures (red arrow) in spongiomicrobialite, well QT-1, depth 6004 m; (i) microfracture filled with bitumen (red arrow), well LT-1, depth 8731 m.

seawater-derived fluids provided large volumes of Mg^{2+} for the formation of the pervasive matrix dolomites during very early diagenesis (Tang et al., 2022).

4.3.4 Cementation

Dolomites are the main cements in the reservoir spaces. Multiphase dolomite cements can be recognized microscopically: fibrous dolomite cement (Cd1), bladed dolomite cement (Cd2), fine-to-medium crystalline dolomite cement (Cd3) and coarse crystalline saddle dolomite cement (Cd4). Cd1 and Cd2 generally have a crystal size of less than 30 μm . They are characterized by

cement crusts of sheet cavities in the microbial carbonates (Fig. 8c–d), particularly in spongiomicrobialite. In some thinsections, phase Cd2 grows over phase Cd1 without optical continuity. Cd3 and Cd4 have larger crystal sizes, varying from 50 to 800 μm , occurring as pore-fillings (Fig. 8e) which may grow upon the bladed cement phase.

Besides dolomite cements, other cements consist of chalcedony, quartz and calcite (Fig. 8e, f). These cements are minor and locally developed.

4.3.5 Fracturing

Fractures are very common in these microbial

carbonates. Tectonic fractures occur in groups with straight shapes (Fig. 8g), some of which are partially filled by clay minerals and cements. Additionally, intersecting microfractures were frequently observed in thin sections (Fig. 8h). Unfilled fractures can provide a route for dissolution fluids and hydrocarbon migration (Fig. 8i), which are important for improving the permeability of the pore systems.

5 Discussion

5.1 Diagenetic sequence

Based on the results described above and combined with the in-situ U-Pb dating age of different dolomite cements (i.e., Cd1 to Cd4) (Yang H X et al., 2020), it is possible to interpret the diagenetic history of these microbial carbonates (Fig. 9). The classification of the diagenetic environment follows the scheme proposed by Moore (2001).

In the marine environment, various microbial mats were deposited in the Late Ediacaran. In this stage, micrite envelopes were the products of micritization due to microbial activities, so thin rims around microbial fabrics (e.g., spongy fabric) can be observed microscopically (Fig. 4h). The sea-level fluctuations resulted in intermittent and transitory exposure. Thereafter, pervasive dolomitization by seawater-derived fluids formed massive dolomites of the Qigebrak Formation during early diagenesis. In the terminal Ediacaran, as the result of the ‘Kalpin movement’, the Aksu area was subject to uplift and subaerially exposed, forming an unconformity on top of the Qigebrak Formation (Shang et al., 2020). Thus, karstification by meteoric water has played a crucial role in forming the caves/vugs below the unconformity, greatly improving the reservoir properties in the upper part of the Qigebrak Formation. After the dissolution, the first

generation of dolomite cement (i.e., Cd1) precipitated in a submarine environment (Ding et al., 2019b) and filled the previous voids, forming the lacy framework fabrics (Figs. 4b, 7d).

The burial environment substantially affected the microbial carbonates after the early stage of diagenesis, with increasing depths and formation temperatures. Bladed dolomite cement (Cd2) precipitated at 542.7 ± 8.0 Ma in a near-surface to shallow burial environment (less than 500 m). With the increase of burial depth, stylolites with associated pressure dissolution occur. The precipitation of fine-to-medium crystalline dolomite cement (Cd3) in the Ordovician has greatly reduced the porosity. During this period, hydrocarbon produced from the Lower Cambrian Yuertusi Formation started to migrate into the pore spaces (Zheng et al., 2018). In the Permian-Triassic, hydrothermal processes occurred locally and resulted in the precipitation of coarse crystalline dolomite cement (Cd4) and quartz, further reducing the reservoir spaces. During the uplift phase from the Jurassic to the present, a large number of structural fractures were formed, due to the release of tectonic stress.

5.2 Pore evolution

As indicated above, the spongiomicrobialite has the best reservoir properties of all the types of microbial carbonates (Figs. 5, 6). Taking this type as an example, the pore evolution processes were reconstructed (Fig. 10a–d).

Observation of thin sections shows that microbial carbonates of the Qigebrak Formation were mainly subjected to two stages of dissolution. The first stage was the fabric-selective dissolution in the syn-depositional period, which was formed by high-frequency sea-level changes and characterized by the occurrence of microbial framework pores (e.g. fenestral pores). The second stage of dissolution was related to the karstification at the end of

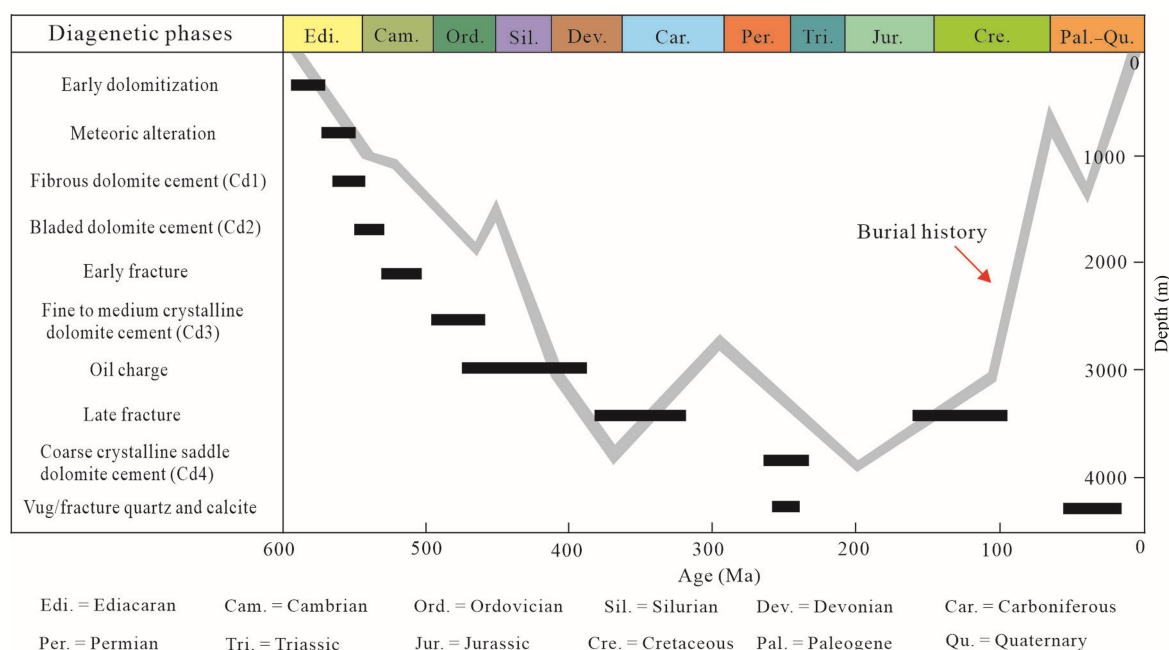


Fig. 9. Diagenetic sequence and burial history of the microbial carbonates in the Qigebrak Formation. Burial history was modified from Chang et al. (2011).

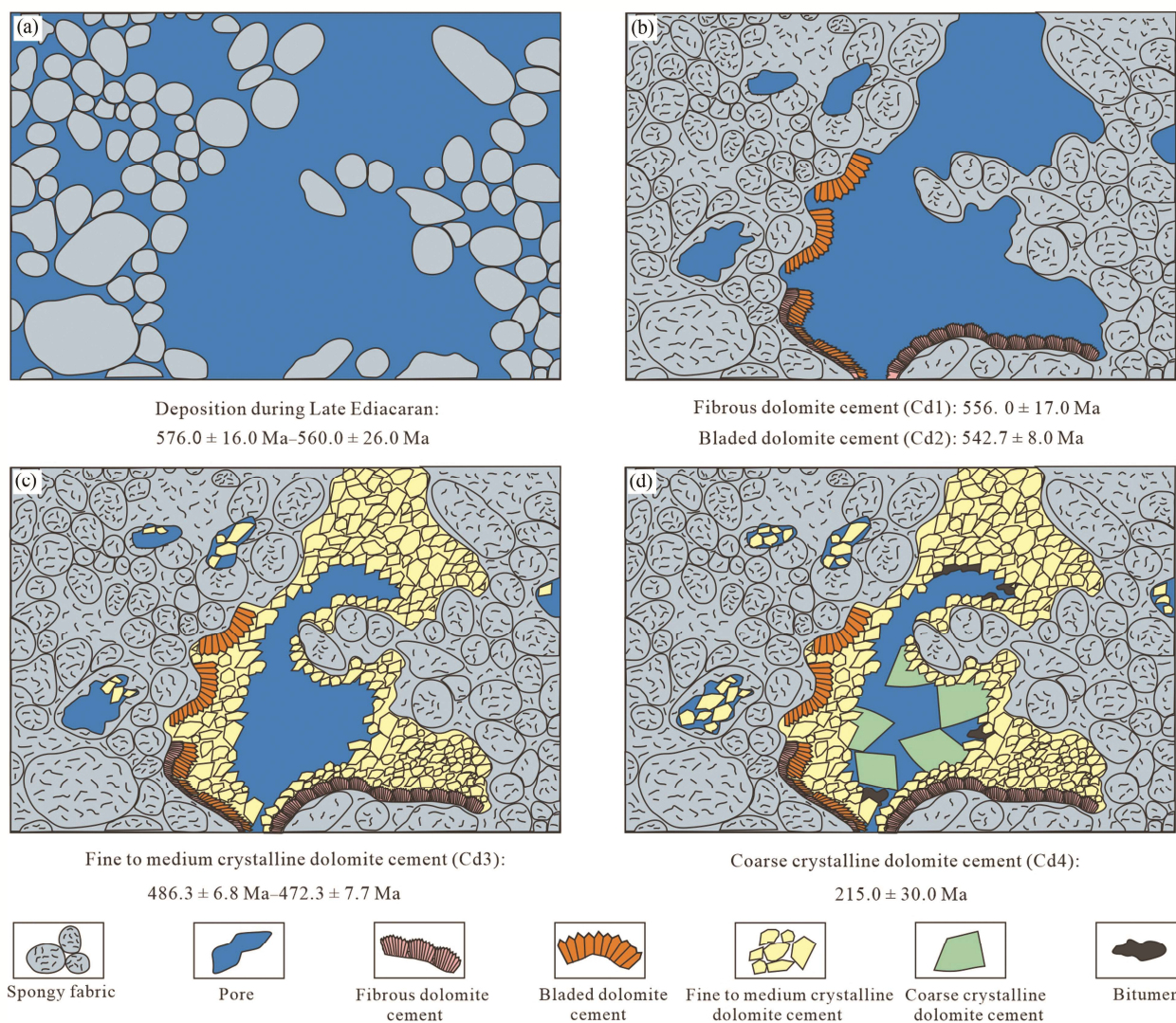


Fig. 10. Pore evolution of spongiomicrobialite in the Qigebrak Formation. The U-Pb dating age of various dolomite cements are from Yang H X et al. (2020).

the Late Ediacaran, secondary pores (e.g., vugs and dissolution-enlarged pores) being the products of this dissolution, which is the predominant pore type. The relatively long-term exposure resulted in a large number of secondary pores in the microbial carbonates. Even though the Qigebrak Formation has experienced a long-term burial phase following deposition, few pores produced by burial fluids can be identified microscopically.

This interpretation was further supported by the U-Pb dating age for the dolomite cements. Yang H X et al. (2020) investigated the age of the matrix and various cements of dolomite samples in the Qigebrak Formation from Xiaonerbrak section using laser in-situ U-Pb dating, concluding that the timing of the Qigebrak Formation deposition could be constrained as being from 576.0 ± 16.0 Ma to 560.0 ± 26.0 Ma. The precise timings for the precipitation of various dolomite cements (i.e., Cd1 to Cd4) are listed in Figure 10. Point-counting porosity data from thin sections show that after the cementation of Cd1 and Cd2, the spongiomicrobialites still had a high porosity

at more than 25%, implying unfilled pores were well-preserved prior to 542.7 ± 8.0 Ma (Fig. 10a–b). However, it seems that the precipitation of Cd3, occurring from 486 ± 6.8 Ma to 472.3 ± 7.7 Ma, was the most significant phase, occluding the pre-existing pores. In this case, the cementation of Cd3 greatly reduced the porosity (Fig. 10c), with residual porosity substantially diminished to 15%. When the Qigebrak Formation was buried to greater depth, intense compaction and the cementation of Cd4 further reduced the porosity (Fig. 10d). Modification of other diagenetic phases were not so obvious. The final porosity is about 6%–8% at present, which is consistent with those of the spongiomicrobialite samples measured for their petrophysical properties (average porosity 6.15%).

As for stromatolites, they experienced similar pore evolution processes to the spongiomicrobialites, the most significant difference being that the laminite fabrics might not have provided the same rigid matrix framework as the spongy fabrics did, thus primary pores in the stromatolites

could be destroyed after long-term burial diagenesis. This might explain the present porosities of stromatolites being relatively lower than spongiomicrobialites (Figs. 5, 6).

In summary, the present reservoir spaces of microbial carbonates were mainly formed in a syn-depositional period and at the end of the Late Ediacaran. After this time, these pores experienced multistage filling and/or cementation phases, although newly-formed reservoir pore spaces were insignificantly low.

5.3 Influence of microbial fabric on pore evolution

The formation of microbial carbonates includes four end-member processes: trapping and binding carbonate sediments, abiotic/inorganic precipitation, biologically-induced calcification and biologically-influenced calcification (Embry and Klovan, 1971; Wright, 1992; Dupraz et al., 2009). Microbial fabrics occur as the building blocks of microbial carbonates, more importantly, forming the initial primary pore that will either be preserved or altered by later diagenetic processes (Sarg et al., 2013; Hubert et al., 2018).

The deposition of various microbial mats leads to the formation of different microbial fabrics. This process would make a difference in the primary pore type and initial porosity in each type of microbial carbonate (Rezende et al., 2013). Specifically, in the studied interval, in spongiomicrobialite, the primary pores are mainly distributed within the spongy fabrics, characterized by mold pores, some of them potentially being further enlarged by meteoric water leaching, so spongy fabric-related pores are the dominant type (Fig. 7a, c). For microbial laminites and stromatolites, reservoir spaces are dominated by fenestral pores, which are mostly distributed in light-colored laminae (Fig. 7b). The laminite fabrics have controlled the distribution and morphologies of these pores, and the fenestral pores being very easily filled by later dolomite cements. These phenomena suggest that even though the Qigebrak Formation has undergone complex diagenetic processes in burial realm, the pore type and pore structure have kept relatively stable, thus the microbial fabrics have possibly controlled the trend of pore evolutionary processes (Yu et al., 2018).

6 Conclusions

The Late Ediacaran microbial carbonates of the Tarim Basin include four types: microbial laminite, stromatolite, spongiomicrobialite and microbial-peloidal wackestone/mudstone. They mainly deposited in a variety of settings in the platform interior, the morphologies of these microbial carbonates pointing to varied depositional environments with different water energy conditions.

The spongiomicrobialite possesses the best reservoir potential of all types of microbial carbonates. Dissolution, compaction, seawater dolomitization, cementation and fracturing are the dominant diagenetic processes. The reservoir spaces of the microbial carbonates were mainly formed in the syn-depositional period and the terminal Ediacaran, subject to fabric-selective dissolution and karst dissolution, respectively. During the burial phase, the cementation of fine-to-medium crystalline dolomite

(Cd3) during the Ordovician was the most significant diagenetic event to reduce the pre-existing porosities. The pore types have kept relatively stable, even though these microbial carbonates experienced long-term diagenetic alteration.

Acknowledgements

This work was financially supported by the National Key Research and Development (R & D) Program of China (2017YFC0603103) and the National Natural Science Foundation of China (U19B6003). We thank Ziwen Jiang for his assistance in microscopic petrographical observations. We are especially grateful for the constructive suggestions from two anonymous reviewers.

Manuscript received Feb. 12, 2022

accepted May 22, 2022

associate EIC: ZHANG Shuichang

edited by Jeffery J. LISTON and FANG Xiang

References

- Bahniuk, A.M., Anjos, S., França, A.B., Matsuda, N., Eiler, J., McKenzie, J.A., and Vasconcelos, C., 2015. Development of microbial carbonates in the Lower Cretaceous Codó Formation (north-east Brazil): Implications for interpretation of microbialite facies associations and palaeoenvironmental conditions. *Sedimentology*, 62: 155–181.
- Braga, J.C., Martin, J.M., and Riding, R., 1995. Controls on microbial dome fabric development along a carbonate-siliciclastic shelf basin transect, SE Spain. *Palaios*, 10: 347–361.
- Burne, R.V., and Moore, L.S., 1987. Microbialites: Organosedimentary deposits of benthic microbial communities. *Palaios*, 2: 241–254.
- Chang, J., Qiu, N.S., Zuo, Y.H., and Li, C.C., 2011. The new evidence on tectonic uplift in Kepingtage area, Tarim Basin: Constraints from (U-Th)/He ages. *Chinese Journal of Geophysics*, 54(1): 163–172 (in Chinese with English abstract).
- Chen, J.T., and Lee, J.H., 2014. Current progress on the geological record of microbialites and microbial carbonates. *Acta Geologica Sinica (English Edition)*, 88(1): 260–275.
- Chen, Z.Q., Tu, C., Pei, Y., Ogg, J., Fang, Y., Wu, S., Feng, X., Huang, Y., Guo, Z., and Yang, H., 2019. Biosedimentological features of major microbe-metazoan transitions (MMTs) from Precambrian to Cenozoic. *Earth-Science Reviews*, 189: 21–50.
- Collins, J.F., Kenter, J.A.M., Harris, P.M., Kuanysheva, G., Fischer, D.J., and Steffen, K.L., 2006. Facies and reservoir-quality variations in the late Viséan to Bashkirian outer platform, rim, and flank of the Tengiz buildup, Precaspian Basin, Kazakhstan. In: Harris, P.M., and Weber, L.J. (eds.), *Giant hydrocarbon reservoirs of the world: From rocks to reservoir characterization and modeling*. AAPG Memoir 88, SEPM Special Publication, 55–95.
- Couradeau, E., Benzerara, K., Gérard, E., Moreira, D., Bernard, S., Brown, G.E., and López-García, P., 2012. An early-branching microbialite cyanobacterium forms intracellular carbonates. *Science*, 336: 459–462.
- Ding, Y., Chen, D.Z., Zhou, X.Q., Guo, C., Huang, T.Y., and Zhang, G.J., 2019a. Tectono-depositional pattern and evolution of the middle Yangtze Platform (South China) during the late Ediacaran. *Precambrian Research*, 333: 105426.
- Ding, Y., Chen, D.Z., Zhou, X.Q., Guo, C., Huang, T.Y., and Zhang, G.J., 2019b. Cavity-filling dolomite speleothems and submarine cements in the Ediacaran Dengying microbialites, South China: Responses to high-frequency sea-level

- fluctuations in an 'aragonite-dolomite sea'. *Sedimentology*, 66: 2511–2537.
- Dunham, R.J., 1962. Classification of Carbonate Rock. AAPG Memoir, 1: 108–121.
- Dupraz, C., Reid, R.P., Braissant, O., Decho, A.W., Norman, R.S., and Visscher, P.T., 2009. Processes of carbonate precipitation in modern microbial mats. *Earth-Science Reviews*, 96: 141–162.
- Embry, A.F., and Klovan, J.E., 1971. A late Devonian reef tract on northeastern Banks Island, N.W.T. *Bulletin of Canadian Petroleum Geology*, 19: 730–781.
- Flügel, E., 2010. *Microfacies of carbonate rocks: Analysis, interpretation and application* (second edition). Berlin: Springer, 745–749.
- Harwood, C.L., and Sumner, D.Y., 2011. Microbialites of the Neoproterozoic Beck Spring dolomite, southern California. *Sedimentology*, 58: 1648–1673.
- He, D.F., Jia, C.Z., Li, D.S., Zhang, C.J., Meng, Q.R., and Shi, X., 2005. Formation and evolution of polycyclic superimposed Tarim Basin. *Oil and Gas Geology*, 26(1): 64–77 (in Chinese with English abstract).
- He, J.Y., Qing, H.R., and Xu, B., 2018. The unconformity-related palaeokarst in the uppermost Ediacaran carbonate rocks in the northwestern Tarim Block, NW China: Implication for sedimentary evolution during the Ediacaran–Cambrian transition. *International Geology Review*, 61: 839–852.
- Hofmann, H., 1973. Stromatolites: Characteristics and utility. *Earth-Science Reviews*, 9: 339–373.
- Hubert, H.L., Rankey, E.C., and Omelon, C., 2018. Organic matter, textures, and pore attributes of hypersaline lacustrine microbial deposits (Holocene, Bahamas). *Journal of Sedimentary Research*, 88: 827–849.
- Jia, C.Z., 1999. Structural characteristics and oil/gas accumulative regularity in Tarim Basin. *Xinjiang Petroleum Geology*, 20(3): 177–183 (in Chinese with English abstract).
- Jiang, L., Hu, S.Y., Zhao, W.Z., Xu, Z.H., Shi, S.Y., Fu, Q.L., Zeng, H.L., Liu, W. and Fall, A., 2018. Diagenesis and its impact on a microbially derived carbonate reservoir from the Middle Triassic Leikoupo Formation, Sichuan Basin, China. *AAPG Bulletin*, 102(12): 2599–2628.
- Kah, L.C., Bartley, J.K., Frank, T.D., and Lyons, T.W., 2006. Reconstructing sea-level change from the internal architecture of stromatolite reefs: An example from the Mesoproterozoic Sulky Formation, Dismal Lakes Group, arctic Canada. *Canadian Journal of Earth Sciences*, 43: 653–669.
- Kenter, J.A.M., Harris, P.M., and Della Porta, G., 2005. Steep microbial boundstone-dominated platform margins—Examples and implications. *Sedimentary Geology*, 178: 5–30.
- Li, F., Deng, J.T., Kershaw, S., Burne, R., Gong, Q.L., Tang, H., Lu, C.J., Qu, H.Z., Zheng, B.S., Luo, S.C., Jin, Z.M., and Tan, X.C., 2021. Microbialite development through the Ediacaran–Cambrian transition in China: Distribution, characteristics, and paleoceanographic implications. *Global and Planetary Change*, 205: 103586.
- Li, P.W., Luo, P., Chen, M., Song, J.M., Jin, T.F., and Wang, G.Q., 2015. Characteristics and origin of the Upper Sinian microbial carbonate reservoirs at the northwestern margin of Tarim Basin. *Oil and Gas Geology*, 36(3): 416–428 (in Chinese with English abstract).
- Li, Y., Jiang, H.X., Wu, Y.S., Pan, W.Q., Zhang, B.S., Sun, C.H. and Yang, G., 2021. Macro-and microfeatures of Early Cambrian dolomitic microbialites from Tarim Basin, China. *Journal of Palaeogeography*, 10(1): 1–20.
- Li, Z.X., and Powell, C.M., 2001. An outline of the palaeogeographic evolution of the Australasian region since the beginning of the Neoproterozoic. *Earth-Science Reviews*, 53: 237–277.
- Lin, C.S., Li, H., and Liu, J.Y., 2012. Major unconformities, tectonostratigraphic framework, and evolution of the superimposed Tarim Basin, Northwest China. *Journal of Earth Science*, 23: 395–407.
- Moore, C.H., 2001. Carbonate reservoirs: Porosity, evolution and diagenesis in a sequence stratigraphic framework. Amsterdam: Elsevier, 1–444.
- Muniz, M., and Bosence, D., 2012. Carbonate platforms in non-marine rift system in the early Cretaceous (Pre-salt) of the Campos Basin, Brazil. Long Beach: AAPG Annual Convention and Exhibition.
- Rezende, M.F., Tonietto, S.N., and Pope, M.C., 2013. Three-dimensional pore connectivity evaluation in a Holocene and Jurassic microbialite buildup. *AAPG Bulletin*, 97: 2085–2101.
- Riding, R., 2000. Microbial carbonates: The geological record of calcified bacterial-algal mats and biofilms. *Sedimentology*, 47: 179–214.
- Riding, R., 2011. The nature of stromatolites: 3,500 million years of history and a century of research. In: *Advances in stromatolite geobiology*. Heidelberg: Springer-Verlag Berlin, 29–74.
- Sarg, J.F., Tānavsuu-Milkeviciene, K., and Humphrey, J.D., 2013. Lithofacies, stable isotopic composition, and stratigraphic evolution of microbial and associated carbonates, Green River Formation (Eocene), Piceance Basin, Colorado. *AAPG Bulletin*, 97: 1937–1966.
- Seckbach, J., and Oren, A., 2010. Microbial mats: Modern and ancient microorganisms in stratified systems. Springer Science and Business Media, 43.
- Shang, Y.X., Gao, Z.Q., Fan, T.L., Wei, D., Wang, Z.Y., and Karubandika, G.M., 2020. The Ediacaran–Cambrian boundary in the Tarim Basin, NW China: Geological data anomalies and reservoir implication. *Marine and Petroleum Geology*, 111: 557–575.
- Shapiro, R.S., 2000. A comment on the systematic confusion of thrombolites. *Palaios*, 15: 166–169.
- Shi, K.B., Liu, B., Tian, J.C., and Pan, W.Q., 2016. Sedimentary characteristics and lithofacies paleogeography of Sinian in Tarim Basin. *Acta Petrolei Sinica*, 37(11): 1344–1360 (in Chinese with English abstract).
- Tang, P., Chen, D.Z., Wang, Y.Z., Ding, Y., El-Shafey, M., and Yang, B., 2022. Diagenesis of microbialite-dominated carbonates in the Upper Ediacaran Qigebrak Formation, NW Tarim Basin, China: Implications for reservoir development. *Marine and Petroleum Geology*, 136: 105476.
- Tucker, M.E., and Wright, V.P., 1990. *Carbonate Sedimentology*. Oxford: Blackwell Science, United Kingdom, 155–156.
- Tull, S.J., 1997. The diversity of hydrocarbon habitat in Russia. *Petroleum Geoscience*, 3: 315–325.
- Turner, S.A., 2010. Sedimentary record of late Neoproterozoic rifting in the NW Tarim Basin, China. *Precambrian Research*, 181: 85–96.
- Wright, V.P., 1992. A revised classification of limestones. *Sedimentary Geology*, 76: 177–185.
- Wu, L., Guan, S.W., Yang, H.J., Ren, R., Zhu, G.Y., Jin, J.Q., and Zhang, C.Y., 2017. The paleogeographic framework and hydrocarbon exploration potential of Neoproterozoic rift basin in northern Tarim Basin. *Acta Petrolei Sinica*, 38(4): 375–385 (in Chinese with English abstract).
- Yang, F., Bao, Z.D., Zhang, D.M., Jia, X., and Xiao, J., 2017. Carbonate secondary porosity development in a polyphase paleokarst from Precambrian system: Upper Sinian examples, North Tarim basin, northwest China. *Carbonates Evaporites*, 32: 243–256.
- Yang, H.J., Chen, Y.Q., Tian, J., Du, J.H., Zhu, Y.F., Li, H.H., Pan, W.Q., Yang, P.F., Li, Y., and An, H.T., 2020. Great discovery and its significance of ultra-deep oil and gas exploration in well Luntan-1 of the Tarim Basin. *China Petroleum Exploration*, 25(2): 62–72 (in Chinese with English abstract).
- Yang, H.X., Hu, A.P., Zheng, J.F., Liang, F., Luo, X.Y., Feng, Y.X., and Shen A.J., 2020. Application of mapping and dating techniques in the study of ancient carbonate reservoirs: A case study of Sinian Qigebrak Formation in northwestern Tarim Basin, NW China. *Petroleum Exploration and Development*, 47(5): 1–12.
- Yu, H.Y., Cai, C.F., Zheng, J.F., Huang, L.L., and Yuan, W.F., 2018. Influence of microbial textures on pore characteristics of microbial dolomites: A case study of Lower Cambrian Xiaerbulake Formation in Keping area, Tarim Basin. *Petroleum Geology and Experiment*, 40(2): 233–243 (in

- Chinese with English abstract).
- Zhai, M.G., 2013. The main old lands in China and assembly of Chinese unified continent. *Science China: Earth Sciences*, 56: 1829–1852.
- Zhang, J., Zhang B.M., and Shan X.Q., 2017. Review and Significance of Microbial Carbonate Reservoirs in China. *Acta Geologica Sinica (English Edition)*, 91(1): 157–158.
- Zhang, X.F., Liu, B., Wang, J.Q., Zhang, Z., Shi, K.B., and Wu, S.L., 2014. Adobe photoshop quantification (PSQ) rather than point-counting: a rapid and precise method for quantifying rock textural data and porosities. *Computers and Geosciences*, 69: 62–71.
- Zheng, J.C., Li, B., Wu, H.Y., Yuan, Q., Liu, Y.L., Xiao, P.C., Li, Q.Q., and Zeng, L., 2018. Study on the thermal history of the source rock and its relationship with hydrocarbon accumulation based on the basin modeling technology: A case of the Yuertusi Formation of Tarim Basin. *Petroleum Geology and Recovery Efficiency*, 25(5): 39–49 (in Chinese with English abstract).
- Zhou, X.Q., Chen, D.Z., Qing, H.R., Qian, Y.X., and Wang, D., 2014. Submarine silica-rich hydrothermal activity during the earliest Cambrian in the Tarim Basin, Northwest China. *International Geology Review*, 56: 1906–1918.
- Zhu, D.Y., Meng, Q.Q., Jin, Z.J., Liu, Q.Y., and Hu, W.X., 2015. Formation mechanism of deep Cambrian dolomite reservoirs in the Tarim Basin, northwestern China. *Marine and Petroleum Geology*, 59: 232–244.
- Zhu, D.Y., Liu, Q.Y., He, Z.L., Ding, Q. and Wang, J.B., 2020. Early development and late preservation of porosity linked to presence of hydrocarbons in Precambrian microbialite gas reservoirs within the Sichuan Basin, southern China. *Precambrian Research*, 342: 105694.

- Zhu, D., Liu, Q.Y., Wang, J.B., Ding, Q., and He, Z.L., 2021. Stable carbon and oxygen isotope data of Late Ediacaran stromatolites from a hypersaline environment in the Tarim Basin (NW China) and their reservoir potential. *Facies*, 67(3): 1–25.

About the first author



TANG Pan, male, born in 1990 in Jingzhou City, Hubei Province. He is a doctoral candidate at the Institute of Geology and Geophysics, Chinese Academy of Sciences. He is currently interested in carbonate diagenesis. E-mail: tangpan2013@126.com.

About the corresponding author



CHEN Daizhao, male, born in 1963 in Shaoyang City, Hunan Province, Ph.D., graduated from the Chinese Academy of Sciences. He is a professor at the Institute of Geology and Geophysics, Chinese Academy of Sciences. He is interested in carbonate sedimentology and diagenesis. E-mail: dzh-chen@mail.iggcas.ac.cn.